Supercooling of the Disordered Vortex Lattice in $Bi_2Sr_2CaCu_2O_{8+\delta}$

C. J. van der Beek,[1] S. Colson,[1] M. V. Indenbom,[1,2] and M. Konczykowski[1]
[1]*Laboratoire des Solides Irradiés, Ecole Polytechnique, 91128 Palaiseau, France*
[2]*Institute of Solid State Physics, 142432 Chernogolovka, Moscow District, Russia*
(Received 10 September 1999)

Time-resolved local induction measurements near the vortex lattice order-disorder transition in optimally doped $Bi_2Sr_2CaCu_2O_{8+\delta}$ crystals show that the high-field, disordered phase can be quenched to fields as low as half the transition field. Over an important range of fields, the electrodynamical behavior of the vortex system is governed by the coexistence of ordered and disordered vortex phases in the sample. We interpret the results as supercooling of the high-field phase and the possible first-order nature of the order-disorder transition at the "second magnetization peak."

PACS numbers: 74.60.Ec, 74.60.Ge, 74.60.Jg

It is now well accepted that the mixed state in type-II superconductors is subdivided into different vortex phases. In clean materials, notably single crystals of the high-T_c cuprates $YBa_2Cu_3O_{7-\delta}$ [1] and $Bi_2Sr_2CaCu_2O_{8+\delta}$ [2–4], the vortex lattice undergoes a first-order transition (FOT) to a flux liquid state without long-range order [5]. The FOT is observed at (high) temperatures at which vortex pinning by crystalline defects is negligible and the vortex system can rapidly relax to thermodynamic equilibrium [3]. It is prolongated into the low temperature regime of nonlinear vortex response by a transition from the weakly pinned low-field vortex lattice to a strongly pinned, disordered high-field vortex phase [4,6,7]. This order-disorder transition is manifest through the so-called "second-peak" feature in magnetic hysteresis loops, a result of the dramatic increase of the sustainable shielding current associated with bulk pinning [4,8–10]. It was proposed that the crossover from the FOT to the second-peak regime constitutes a critical point in the phase diagram [3,11], which in $Bi_2Sr_2CaCu_2O_{8+\delta}$ would lie near $T \approx 40$ K. In more dirty type-II superconductors the FOT and the critical point are absent, and the critical current "peak effect" is found at temperatures up to T_c [12]. The peak is often accompanied by strongly history-dependent dynamical behavior of the vortex system at fields and temperatures just below it, suggesting that a first-order transition lies at its origin [13–15].

Among the above-mentioned materials the layered superconductor $Bi_2Sr_2CaCu_2O_{8+\delta}$ has a specific interest: its high Ginzburg number $\mathrm{Gi} \sim 0.01$ means that vortex lines are extremely sensitive to thermal and static fluctuations and that the FOT and second-peak lines are depressed to inductions lower than 1 kG. The local induction B and flux dynamics around the transition can then be accurately measured using local Hall-array magnetometry [3,4,9,10] and magneto-optics. The latter technique was recently used to image the separation of the vortex system near the FOT in $Bi_2Sr_2CaCu_2O_{8+\delta}$ into coexisting lattice and liquid phases [16]. In this Letter, we image the flux dynamics and the coexistence of the two *pinned* vortex phases in $Bi_2Sr_2CaCu_2O_{8+\delta}$ near the disordering transition at the "second peak." In particular, we find that the disordered phase can be quenched to flux densities that are nearly half that at which it exists in equilibrium. We interpret our results in terms of supercooling of the high-field phase. This suggests that the order-disorder transition at the second peak is of first order, and that it is the "true" continuation of the FOT in the regime of slow vortex dynamics. By implication, we propose that a putative critical point lies at a temperature not exceeding 14 K.

The experiments were performed on an optimally doped $Bi_2Sr_2CaCu_2O_{8+\delta}$ single crystal ($T_c = 90$ K) of size $640 \times 230 \times 25\ \mu\mathrm{m}^3$, grown at the University of Tokyo using the traveling-solvent floating zone technique, and selected for its uniformity. Previous experiments on this crystal using the Hall-probe array technique have revealed the disordering transition of the vortex lattice to occur at $B_{\mathrm{sp}} = 380$ G [10]. We have visualized the flux density distribution at inductions B close to the transition using the magneto-optical technique [17]. A ferrimagnetic garnet indicator film with in-plane anisotropy is placed directly on top of the crystal, and observed using linearly polarized light. The reflected light intensity, observed through an analyzer oriented nearly perpendicularly to the polarization direction, corresponds to the local value B_z of the induction component perpendicular to the crystal (and to the garnet). An external magnetic field H_a is applied perpendicularly to the crystal plane, using a symmetrically positioned split-coil magnet (with $L/R = 21$ ms) driven by a fast bipolar power supply (roll-off frequency $\sim$40 kHz).

Figure 1(a) shows a magneto-optical image of the crystal after zero-field cooling to $T = 24.6$ K and the slow ramp of H_a to 486 G. There is a bright belt around the crystal edge, corresponding to a region of high B_z gradient, and, visible under the sawtoothlike magnetic double-domain-wall structure in the garnet, an inner region with little contrast, indicating a plateau in the local induction. The axes of the sawtooth structures are located where the induction component parallel to the garnet film, $B_{\parallel}$, vanishes [18], in this case at the boundary between regions of zero and nonzero screening current in the crystal. There is a large screening current in the regions limited by the "upper" and "lower" crystal edges and the domain walls

 0031-9007/00/84(18)/4196(4)$15.00

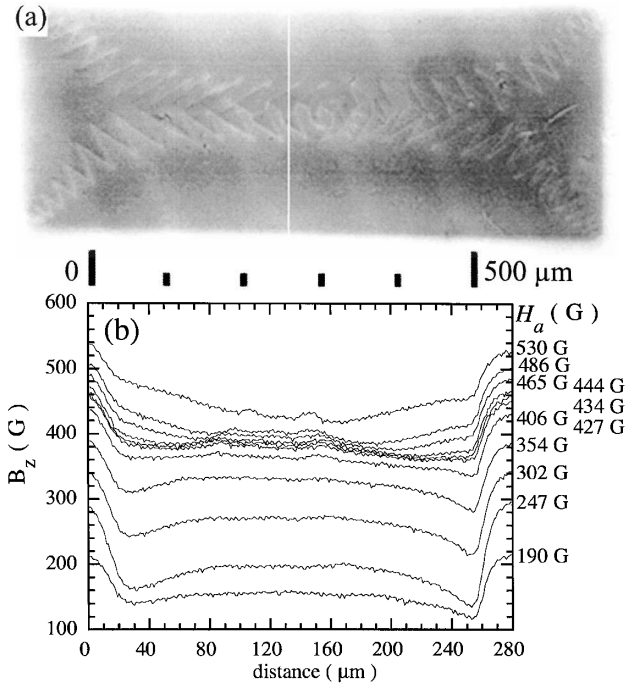

FIG. 1. (a) Magneto-optical image of the flux distribution on the surface of the $Bi_2Sr_2CaCu_2O_8$ crystal after zero-field cooling to $T = 24.6$ K and the slow ramp of the applied field to $H_a = 486$ G. (b) Profiles of the magnetic induction B_z at successive H_a values during the field ramp, taken along the white line in (a). The step in B_z at the crystal edges is the result of the edge barrier current [20]. The small irregularities in the center correspond to magnetic domain walls in the garnet film, visible as the "sawtooth" structures in (a).

in the garnet; in the "bright belt," it produces a gradient in B_z, while near the domain walls it leads to a gradient only of $B_\parallel$ (see also Ref. [19], Fig. 12). Calibration of the intensity shows that the plateau induction equals that expected at the transition, $B_{sp} = 380$ G.

The evolution of the B_z profiles at successive values of H_a during the ramp is shown in Fig. 1(b). At small fields, one has a comparatively large step in the induction at the crystal edges, and a dome-shaped flux distribution in the crystal interior. Such profiles occur when the screening current, due to an edge barrier against vortex entry, is much greater than the bulk current, which is the result of vortex pinning [20,21]. The domelike profile moves up to higher induction values as field is increased; its evolution stops when, in the crystal center, B_z reaches $B_{sp} = 380$ G (for $H_a = 427$ G). As H_a is increased further, the flux profile flattens out, i.e., B_z becomes constant throughout the crystal as the high-field vortex phase spreads outward from the crystal center. As a result, the slope $\partial B_z/\partial H_a$ becomes equal to the Meissner slope [10]. At $H_a = 444$ G, the whole crystal is in the high-field state, and new flux (vortices) penetrates from the edges; it cannot, however, accumulate in the crystal center but adopts the linear gradient characteristic of the pinning-induced critical state [22]. This indicates that, at this temperature, field, and field ramp rate, the pinning current is comparable to or greater than the edge current, giving rise to the "second-peak feature" in the magnetic moment [4,6,10].

Figure 2(a) shows the relaxation of the flux profile after a rapid decrease of H_a from 500 to 120 G, at $T = 23$ K. The flux profile before the field decrease is similar to that in Fig. 1 for $H_a = 486$ G: the "critical state" fronts of the high-field phase have not yet penetrated the whole crystal so that the induction in the crystal center is nearly constant: $B_z \gtrsim B_{sp}$; the internal induction is lower than the applied field because of the combined screening by the edge barrier current [20,21] and by the high-field phase. When H_a is suddenly decreased, the sample initially fully screens the field change ($t = 0.16$ s). From $t \gtrsim 0.32$ s onwards, vortices leave the sample. The flux profiles display three distinct linear sections with different gradients, corresponding to three mechanisms opposing vortex motion and exit. The gradient nearest to the edges corresponds to the barrier current [20,21]; the two gradients in the bulk correspond to the (rapidly decaying) screening current in the low-field vortex lattice phase and the (nearly constant) current in the high-field disordered vortex phase, respectively. The phase transformation line, at which one passes from the low-field to the high-field current, progressively

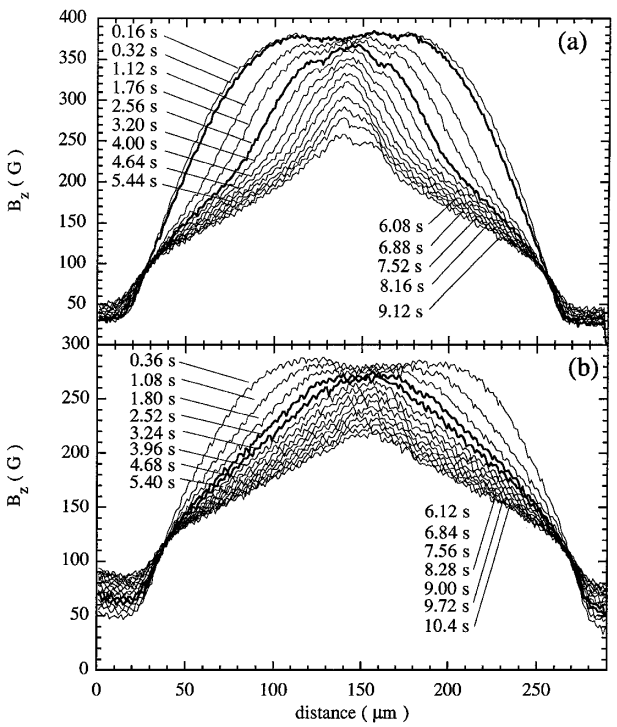

FIG. 2. (a) Relaxation of the flux profile at $T = 23.0$ K after the application of an external field $H_a^{max} = 500$ G and its successive rapid decrease to 120 G. One observes three slopes $\partial B_z/\partial x$, corresponding to the edge current (near 30 and 260 μm) [20], and to bulk screening currents in the low-field and high-field vortex phases, respectively. (b) The same as (a), but after field cooling from $T = 28$ K in $H_a^{max} = 383$ G. Now there are two linear sections corresponding to the edge current and the relaxing critical state established in the low-field phase *only*.

moves to the crystal center, until the whole crystal is in the low-field phase at $t \gtrsim 10$ s. We note that these features are not observed if one prepares a similar initial flux profile with a central plateau of $B_z < B_{sp}$ [Fig. 2(b)]. There are then only *two* distinct gradients corresponding to the edge barrier and the screening current in the low-field phase. These results unambiguously demonstrate that the region of constant flux density B_{sp} in the sample center, obtained during a slow field ramp (Fig. 1), is in the high-field phase; namely, it responds to an external field perturbation by developing the corresponding screening current. Moreover, the current at any point in the crystal *depends on the history* of the vortex system. This is well seen at, e.g., 100 μm and $B_z = 250$ G: if this induction is attained by a quench from the high-field phase, the current is equal to that usually observed for $B_z > B_{sp}$. If, during the experiment, the vortex system did not undergo the phase transformation to the disordered state, a current characteristic of the low-field phase is observed.

Note that the central part of the crystal (Fig. 2) that exhibits the electrodynamic response characteristic of the high-field disordered phase does so at inductions well below B_{sp}, at which this appears under quasiequilibrium conditions (as in Fig. 1). Apparently, when the field is rapidly decreased, flux exit through the relaxation of the low-field vortex lattice around the sample periphery occurs much faster than vortex motion through the phase boundary. Because of this, the high-field phase is quenched: here, to inductions nearly half B_{sp}. A similar situation occurs if one rapidly increases the magnetic field from zero to a value much above B_{sp} (Fig. 3). Again, the crystal initially screens the field change perfectly. When vortices enter the crystal, they are in the disordered state. Only when they move sufficiently far into the interior does the phase

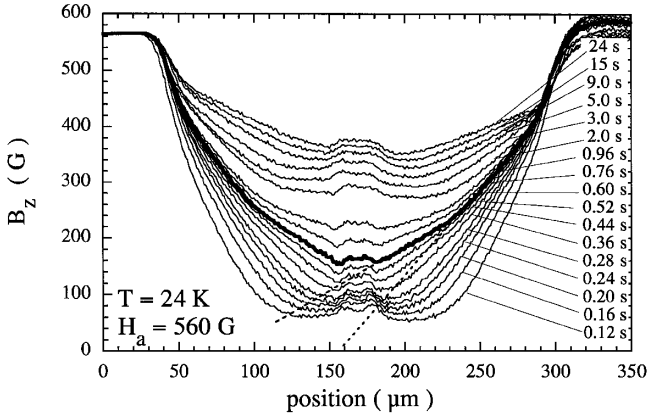

FIG. 3. Relaxation of the flux profile on the crystal surface at $T = 24.0$ K, after the sudden application of an external field $H_a^{max} = 560$ G. For $t > 0.44$ s, the profiles display three slopes $\partial B_z/\partial x$, corresponding to the surface barrier current, and bulk screening currents in the high-field (outer) and low-field (inner) vortex phases, respectively. This is best seen at $t = 0.60$ s (thick line). The irregularities near the center are again due to the domain walls in the garnet film.

transformation to the ordered vortex lattice state take place. The formation of the critical state and the ensuing decrease of the induction, from $B_z \approx \mu_0 H_a > B_{sp}$ near the edge to $B_z \ll B_{sp}$ near the center, impose the presence of the phase transformation line in the sample interior. This is visible in Fig. 3 as the change in $\partial B_z/\partial x$ near 90 and 240 μm. The induction at which the transformation takes place is again lower than B_{sp}, i.e., the high-field phase is now quenched as it penetrates from the sample edge, in this case to an induction $\sim$200 G. As the induction gradient in the high-field phase relaxes due to thermally activated flux motion, the phase transformation line moves from the crystal edges towards the crystal center. In contrast to the dramatic quenching of the disordered phase, we did not, in any experiment, obtain unambiguous indications that the low-field state can be prepared at $B > B_{sp}$.

The above observations have important implications for the vortex phase diagram in $Bi_2Sr_2CaCu_2O_{8+\delta}$ and other layered superconductors. First of all, it is shown that the phase boundary between the low-field lattice phase and the high-field disordered vortex phase is, to within our spatial resolution ($\sim$10 μm), sharp, and that its position can be readily identified by the difference in shielding current density developed by the two phases after a field pertubation. The phase transformation line can, depending on the ratio of these currents, move inwards from the crystal edge, which happens at relatively low temperature or large field sweep rates (Figs. 2 and 3), or outwards from the crystal center, at higher temperatures near the reported "critical point" [3] or during slow field ramps (such as in Fig. 1). In the latter case, any small "external" field perturbation is screened by the high current developed by the disordered vortex phase, so that the induction in the crystal center is held constant and equal to B_{sp} (as in Fig. 1). This notably holds for the discontinuous change of the equilibrium flux density ΔB, associated with the entropy change $\Delta S = \Delta B \partial H_m/\partial T$ at the FOT [3] (H_m is the FOT field), which apparently vanishes at $T \sim 40$ K. Our results give a natural explanation for this, without the need to invoke the presence of a critical point in the phase diagram: ΔB cannot be observed, because it is perfectly screened by the pinning "critical" current developed in the disordered high-field phase. In other words, thermodynamic equilibrium can no longer be achieved, because, for $T \lesssim 40$ K [23], the high-field phase is pinned on the typical experimental time scale. The extra vortices needed to satisfy the constitutive relation $B(H)$ cannot enter the region where the high-field phase is present.

Further support for the absence of a critical point near 40 K is given by the quenching experiments of Figs. 2(a) and 3. The flux distributions shown in these plots correspond to the coexistence of the ordered low-field vortex lattice state and the disordered high-field phase. The latter is *metastable* since it exists at inductions that are much smaller than B_{sp}. We interpret this observation as

supercooling of the disordered state, which in turn suggests that the transition at B_{sp} is of first order. Further, the continuity with the high-temperature FOT [4] implies that it is simply the continuation of the "lattice-to-liquid" transition into the regime of slow vortex dynamics. The observation of the present features at temperatures down to 14 K, below which the second peak cannot be observed at ordinary experimental time scales, means that, if a critical point exists, it should lie *below* 14 K. This would be in agreement with the vortex glass transition line of Ref. [24], the low-field extrapolation of which was found to intercept B_{sp} around the same temperature.

We point out that the possibility of phase coexistence should be taken into account in magnetic relaxation experiments in the peak effect region, especially those triggered by a decrease in the applied magnetic field. In such experiments, the decay rate of the global magnetic moment and of the local induction will be determined by no less than four contributions: the relaxation of the surface barrier current, flux creep in the low-field and high-field vortex phase, and the rate at which the vortex lattice recrystallizes at the phase transformation line. At temperatures below 20 K, these processes become slow and similarly impede flux transport. Supercooling of a disordered vortex phase has been previously observed in other type-II superconductors such as α-Nb_3Ge [13] and $NbSe_2$ [14]. The anomalous flux dynamics observed in the field regime close to but below the critical current peak [15] may find a natural explanation in the "asymmetric" vortex response and flux profiles introduced in transport measurements by phase coexistence and the supercooling phenomenon.

In conclusion, we have visualized the flux distribution in the second-peak regime in $Bi_2Sr_2CaCu_2O_8$. The peak effect feature, the fact that $\partial M/\partial H_a = -1$ below the peak, and the vanishing of ΔB, associated with the FOT at $T \sim 40$ K, are the result of the pinning current in the high-field phase, which prohibits flux entry into this phase until the phase transformation is complete. We have observed supercooling of the high-field disordered vortex system to fields nearly half the phase transformation field B_{sp}. The results suggest that the vortex order-disorder transition at the second peak in $Bi_2Sr_2CaCu_2O_8$ is first order, and that any critical point in the phase diagram lies below 14 K.

We thank N. Motohira for providing the samples, and M. V. Feigel'man, P. H. Kes, A. Soibel, A. Sudbø, and E. Zeldov for fruitful discussions.

[1] H. Safar *et al.,* Phys. Rev. Lett. **69,** 824 (1992); W. K. Kwok *et al.,* Phys. Rev. Lett. **69,** 3370 (1992).
[2] H. Pastoriza *et al.,* Phys. Rev. Lett. **72,** 2951 (1994).
[3] E. Zeldov *et al.,* Nature (London) **375,** 373 (1995).
[4] B. Khaykovich *et al.,* Phys. Rev. Lett. **76,** 2555 (1996).
[5] R. Cubitt et al., Nature (London) **365,** 410 (1993).
[6] R. Cubitt *et al.,* Physica (Amsterdam) **235C–240C,** 2583 (1994).
[7] T. Nishizaki, T. Naito, and N. Kobayashi, Physica (Amsterdam) **282C–287C,** 2117 (1997); K. Deligiannis *et al.,* Phys. Rev. Lett. **79,** 2121 (1997).
[8] N. Chikumoto *et al.,* Phys. Rev. Lett. **69,** 1260 (1992).
[9] D. Majer, E. Zeldov, H. Shtrikman, and M. Konczykowski, in *Coherence in High Temperature Superconductors,* edited by G. Deutscher and A. Revcolevschi (World Scientific, Singapore, 1996).
[10] S. Berry *et al.,* Physica (Amsterdam) **282C–287C,** 2259 (1997).
[11] H. Safar *et al.,* Phys. Rev. Lett. **70,** 3800 (1993).
[12] P. Koorevaar *et al.,* Phys. Rev. B **42,** 1004 (1990); S. Bhattacharya and M. J. Higgins, Phys. Rev. Lett. **70,** 2617 (1993); G. D'Anna, M.-O. André, and W. Benoit, Europhys. Lett. **25,** 539 (1994); R. Modler *et al.,* Phys. Rev. Lett. **76,** 1292 (1996); D. Giller *et al.,* Phys. Rev. Lett. **79,** 2542 (1997); M. Pissas *et al.,* Phys. Rev. B **59,** 12 121 (1999); S. Anders *et al.,* Phys. Rev. B **59,** 13 635 (1999).
[13] R. Wördenweber and P. H. Kes, Phys. Rev. B **34,** 494 (1986).
[14] W. Henderson, E. Y. Andrei, M. J. Higgins, and S. Bhattacharya, Phys. Rev. Lett. **77,** 2077 (1996); S. B. Roy and P. Chaddah, J. Phys. Condens. Matter **9,** L625 (1997); G. Ravikumar *et al.,* Phys. Rev. B **57,** R11 069 (1998); S. S. Banerjee *et al.,* Phys. Rev. B **58,** 995 (1998).
[15] W. Henderson, E. Y. Andrei, and M. J. Higgins, Phys. Rev. Lett. **81,** 2352 (1998).
[16] A. Soibel *et al.* (to be published).
[17] L. A. Dorosinskiĭ *et al.,* Physica (Amsterdam) **203C,** 149 (1992).
[18] M. V. Indenbom *et al.,* Physica (Amsterdam) **226C,** 325 (1994).
[19] E. H. Brandt, Phys. Rev. B **54,** 4246 (1996).
[20] M. V. Indenbom *et al.,* in *Proceedings of the Seventh International Workshop on Critical Currents in Superconductors, Alpbach, Austria, 1994,* edited by H. W. Weber (World Scientific, Singapore, 1994).
[21] E. Zeldov *et al.,* Phys. Rev. Lett. **73,** 1428 (1994).
[22] C. P. Bean, Phys. Rev. Lett. **8,** 250 (1962).
[23] D. Fuchs *et al.,* Phys. Rev. Lett. **80,** 4971 (1998).
[24] C. J. van der Beek *et al.,* Physica (Amsterdam) **195C,** 307 (1992).